NASA TECHNICAL NOTE

QUANTUM THEORY OF A PARTICLE-OSCILLATOR COLLISION APPLIED TO GAS-SURFACE INTERACTIONS AT CRYOGENIC TEMPERATURES

by Jerry D. Smith

Lewis Research Center
Cleveland, Ohio

QUANTUM THEORY OF A PARTICLE-OSCILLATOR COLLISION APPLIED

TO GAS-SURFACE INTERACTIONS AT CRYOGENIC TEMPERATURES

By Jerry D. Smith

Lewis Research Center
Cleveland, Ohio

ABSTRACT

The Schrödinger equation was solved numerically for a one-dimensional collision between a harmonic oscillator and a particle, with a rectangular trapping potential. General solutions were sums of states, each a product of a particle wave function and an oscillator wave function. A correlation was suggested between probability current densities for states within the well and sticking of gas atoms on surfaces, where sticking is regarded as arising from multiple collisions. Energy accommodation coefficients were formulated and compared with helium-tungsten experiments for the temperature range 20 to 120 K. The theory underestimates the accommodation coefficient at lower temperatures and overestimates it at higher temperatures. Results indicate that only approximate qualitative predictions of the coefficient are possible with this simplified model.

QUANTUM THEORY OF A PARTICLE-OSCILLATOR COLLISION APPLIED

TO GAS-SURFACE INTERACTIONS AT CRYOGENIC TEMPERATURES

by Jerry D. Smith

Lewis Research Center

SUMMARY

A mathematical model of the interaction of an inert gas atom with a clean cold surface of a solid is proposed. The model is a one-dimensional collision between a particle acting as the gas atom and a simple harmonic oscillator acting as a surface atom. The interaction potential between the two is taken as hard sphere, with a rectangular well in front of the infinite wall. Two regions are created: the well region, where the particle-oscillator separation distance is less than a certain value, and the region outside the well, where the separation exceeds that value.

The solutions to the Schrödinger equations in the two regions are written as sums of component states. Each such state is a product of an unknown coefficient, a particle exponential wave function, and a harmonic oscillator wave function. Boundary conditions are applied, and the unknown coefficients are derived numerically. Probability current densities for component states neighboring a low initial oscillator state are calculated in the two regions for helium and neon on tungsten.

A gas-surface interaction is simulated by an ensemble of particle-oscillator systems. A correlation is suggested between the sum of probability current densities within the well and sticking of gas atoms on a surface. This sum is physical mass flux in one direction. We interpret sticking as arising from a gas atom making multiple collisions with a surface atom. An increase of particle flux within the wells is indicated by the probability current density sum within the wells exceeding the initial incoming density.

Outside the well, transition probabilities are derived from current densities. Then, microscopic energy accommodation coefficients are formulated, suitably averaged, and compared with helium-tungsten experiments for the temperature range 20 to 120 K. The theory underestimates the accommodation coefficient at the lower temperatures and overestimates it at the higher temperatures. Results indicate that only approximate qualitative predictions of the coefficient are possible with this simplified model.

INTRODUCTION

Variations of the present particle-oscillator collision model have been applied before to rarefied gas-surface interactions. The particle-oscillator collision is a reasonable beginning because, for free molecular flow, momentum and energy transfer in a gas-surface interaction depend entirely on the nature of the collisions of individual gas atoms with surface atoms (ref. 1). The model in the present treatment is a one-dimensional collision between a simple harmonic oscillator simulating one of the atoms comprising the surface of the solid, and a particle acting as the gas atom, with a hard sphere interaction potential modified by a rectangular well between the oscillator and the particle.

This model and its mathematical treatment are based on the treatment given by Shuler and Zwanzig (ref. 2) for a similar model. They used only a hard sphere interaction potential (no well) and calculated oscillator transition probabilities. Using a computer solution of the Schrödinger equation, they showed that multiphonon energy exchange can have appreciable probability for certain initial incoming particle energies. This contradicts the one-phonon-selection rule evolved in perturbation treatments of particle-oscillator models (e.g., Devonshire, ref. 3). This one-phonon rule has been shown inadequate to explain condensation of gases on surfaces (ref. 2).

Gilbey used the same model as Shuler and Zwanzig, in a classical and quantum treatment of gas-solid energy exchange (ref. 4). His calculation procedure necessitated a choice of low particle-to-oscillator mass ratio and high particle-to-oscillator energy ratio. Secrest and Johnson used an exponential repulsion interaction potential in their collision model (ref. 5). They calculated transition probabilities using the method of amplitude density functions. Jackson and Mott (ref. 6), Castellan and Hulburt (ref. 7), and Widom (ref. 8) give special approximate analytical solutions for impulsive inelastic collisions.

Of the previous models, only Devonshire's (ref. 3) uses a trapping interaction potential which allows the particle to be found in a bound state near the oscillator. Devonshire's model uses a Morse potential. The previous treatments, including Devonshire's, yield only asymptotic forms of the wave function as the particle approaches $+\infty$ after the interaction. The objective of these previous treatments was to formulate transition probabilities or accommodation coefficients; therefore, primary interest lay in the final state of the system. In contrast, the present treatment yields solutions in a well region near the oscillator. And it does not require assumptions in the mathematical development either about the relative magnitudes of the particle and oscillator coordinates, or about relative magnitudes of initial particle energy, initial oscillator energy, and interaction potential well depth.

Diestler and McKoy (ref. 9) recently presented a general method for the quantum-mechanical treatment of the inelastic collision of composite particles. Their method

could include the Shuler-Zwanzig (ref. 2) and Secrest-Johnson (ref. 5) models, among others, as special cases. However, to adapt the formalism of Diestler and McKoy to the present model, one would have to require that (1) the total wave function vanish when the oscillator coordinate exceeds some particular value, and (2) that the interaction potential vanish when the particle coordinate exceeds some other particular value. Condition (2) defines their asymptotic region. The interaction potential of the present report vanishes when the difference between the oscillator and particle coordinates exceeds some given value. And condition (1) is not required in the present treatment. Furthermore, and more important, although Diestler and McKoy can use a trapping interaction potential, they can derive Schrödinger equation solutions only in their asymptotic region, not in our interaction region (the rectangular well).

Sugawara gave a quantum-mechanical theory of adsorption using basically the same model proposed in the present study (ref. 10). But he allowed a single group of phonons of identical energy to leave the particle-oscillator system at a definite time during the interaction. He then derives an expression for the probability of finding the gas particle in a trapped state immediately after this energy release. However, he was not able to verify, with any experimental comparisons, that either this mechanism of energy release to the crystal or the various approximations introduced in his time-dependent perturbation treatment were justified.

The present model also does not now yield sticking coefficients to be compared with experiments. We only propose a different outlook on the quantum mechanics of trapping a gas atom on a surface: linking the multiple collisions that occur when a gas particle resides in the vicinity of a surface atom to the particle probability current density in that vicinity. The model, however, does yield simply formulated energy accommodation coefficients. But the results for helium on tungsten indicate that only approximate qualitative predictions can be made with this simplified model.

MODEL

The incident gas atom interacts along the line of centers with a rotationless harmonic oscillator, as shown in figure 1. There are several potentials which could be used to describe the physical interaction between the particle and the oscillator. Such potentials are attractive when the interatomic separation is large and repulsive when the separation is small. A hard-sphere potential modified by a rectangular well in front of the infinite wall (see fig. 2) was chosen because then the Schrödinger equation remains separable in the interaction region.

In appendix B, values of the well width b and well depth V_1 were chosen so that the rectangular well potential would approximate a Morse potential. And for this approxima-
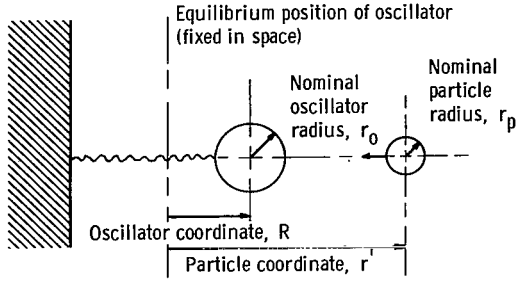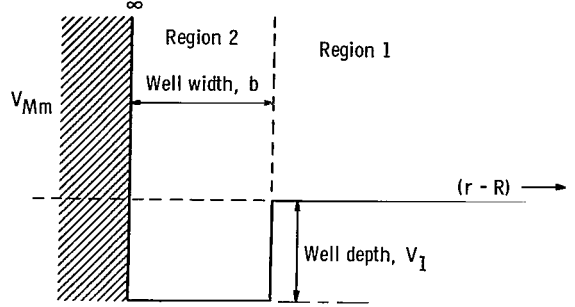
Figure 1. – Particle-oscillator interaction.

Figure 2. – Rectangular interaction potential V_{Mm}. Coordinate r is linearly related to particle coordinate r' (see appendix B), and R is oscillator coordinate.

tion, the Morse potential parameters given by Goodman for rare gas atom - metallic atom combinations were used (ref. 11). The coordinate r in figure 2 is linearly related to the actual particle coordinate r' and is introduced to facilitate subsequent equations (see appendix B). The Schrödinger equations are invariant to this linear transformation.

In terms of the coordinates r and R, the Schrödinger equation in region 1 (r - R $\geq$ b) is

$$\left(- \frac{\hbar^2}{2M} \frac{\partial^2}{\partial R^2} + \frac{1}{2} M\omega^2 R^2 - \frac{\hbar^2}{2m} \frac{\partial^2}{\partial r^2}\right)\Psi_1(r, R) = E(1)\Psi_1(r, R) \tag{1}$$

and in region 2 (0 $\leq$ r - R $\leq$ b) is

$$\left(- \frac{\hbar^2}{2M} \frac{\partial^2}{\partial R^2} + \frac{1}{2} M\omega^2 R^2 - \frac{\hbar^2}{2m} \frac{\partial^2}{\partial r^2} - V_1\right)\Psi_2(r, R) = E(2)\Psi_2(r, R) \tag{2}$$

All symbols are defined in appendix A.

Equations (1) and (2) are separable. The most general solutions to these equations are linear combinations of harmonic oscillator wave functions, $\psi_n(R)$, with oscillator energy $E_{osc} = \left(n + \frac{1}{2}\right)\hbar\omega$, n = 0, 1, ..., and free particle wave functions:

$$\Psi_1(r, R) = A_j\psi_j(R)\exp\left\{- \frac{i[p(j)]r}{\hbar}\right\} + \sum_{f=0}^{\infty} B_f\psi_f(R)\exp\left\{+ \frac{i[p_1(f)]r}{\hbar}\right\} \tag{3}$$

4

$$\Psi_2(r, R) = \sum_{f=0}^{\infty} \psi_f(R) \left(C_f \exp\left\{ -\frac{i[p_2(f)]r}{\hbar} \right\} + D_f \exp\left\{ +\frac{i[p_2(f)]r}{\hbar} \right\} \right) \tag{4}$$

The indices j and f denote initial and final states of the oscillator, respectively. Particle momentum is given by energy conservation in the two regions:

Region 1:

$$\frac{[p_1(f)]^2}{2m} + \left(f + \frac{1}{2}\right)\hbar\omega = \frac{[p(j)]^2}{2m} + \left(j + \frac{1}{2}\right)\hbar\omega \tag{5}$$

Region 2:

$$\frac{[p_2(f)]^2}{2m} + \left(f + \frac{1}{2}\right)\hbar\omega - V_1 = \frac{[p(j)]^2}{2m} + \left(j + \frac{1}{2}\right)\hbar\omega \tag{6}$$

Now, in the total wave functions, states for which $p_1(f)$ and $p_2(f)$ are imaginary are included. These nonphysical states arise when f is large, as can be seen from equations (5) and (6). They must be included in the most general solutions, because without them all the boundary conditions cannot be satisfied. Briefly, the omission of such states would lead to an infinite number of linear equations in a finite number of unknowns, which cannot, in general, be solved. (This set of equations would differ from eqs. (17) to (20) only by having finite summations over states f, instead of infinite summations.)

The notation $p_1(f)$ and $p_2(f)$ is used to indicate that, in calculating $p_1(f)$ and $p_2(f)$ from equations (5) and (6), the positive root is always chosen, whether it is real or imaginary. Doing this ensures that each possible component state is included in the general solutions just once. The initial state appears as the first term in $\Psi_1(r, R)$. Writing the general solutions as shown herein makes the physical meaning of the various component states clear; particle motion to the left or right is implied by negative and positive values of real momentum, respectively.

The boundary conditions are

$$\Psi_2(R, R) = 0 \tag{7}$$

$$\frac{\partial}{\partial R} \Psi_1(r, R)\bigg|_{r-R=b} = \frac{\partial}{\partial R} \Psi_2(r, R)\bigg|_{r-R=b} \tag{8}$$

$$\frac{\partial}{\partial r} \Psi_1(r, R)\bigg|_{r-R=b} = \frac{\partial}{\partial r} \Psi_2(r, R)\bigg|_{r-R=b} \tag{9}$$

$$\Psi_1(r, R)\bigg|_{r-R=b} = \Psi_2(r, R)\bigg|_{r-R=b} \tag{10}$$

The first condition (eq. (7)) is the only one that can be imposed properly at the infinite wall.

It is important to note that the boundary conditions are imposed on the total system wave functions. The only energy quantization that occurs is the well-known $E_{osc} = \left(n + \frac{1}{2}\right)\hbar\omega$ as oscillator energy. This quantization arises only be requiring the wave functions to be bounded everywhere and approach zero as $R \to \infty$. The only requirement for particle momentum is that the corresponding energy satisfy energy conservation. To evolve the familiar energy levels for a particle in a well, one would have to impose function and derivative continuity on parts of the total system wave functions, namely, the free particle exponentials, and this is incorrect. Since the total system Hamiltonians in both regions do not depend on time explicitly, a time-independent formulation is possible, and the total system energy is constant. However, because of energy exchanges with the oscillator, particle energy is not constant in time. Therefore, previous elementary time-independent particle-in-well treatments are inapplicable.

The mathematical procedure introduced by Jackson and Mott (ref. 6) and used by Shuler and Zwanzig (ref. 2) will be used here. The general objective is to evolve a set of simultaneous linear equations which can be solved by computer for accurate values of the lower ordered unknowns B_f, C_f, and D_f (i.e., those having low values of f). These values are used to calculate probability current densities for the lower ordered states:

$$\frac{p_1(f)}{m} |B_f|^2$$

$$\frac{p_2(f)}{m} |C_f|^2$$

$$\frac{p_2(f)}{m} |D_f|^2$$

The oscillator will be given an initial low state, $j = 0, 1, 2$, and sometimes 3, approximately corresponding to a low wall temperature, as seen from appendix E. Interest naturally centers on transitions to neighboring low states. The initial incoming density is $[p(j)/m]|A_j|^2$, and A_j is taken equal to 1.

It will be convenient to nondimensionalize by expressing all energies in terms of $\hbar\omega$ and all lengths in terms of the characteristic harmonic-oscillator length $\alpha^{-1} = (M\omega/\hbar)^{-1/2}$ by using the following relations:

$$\left.\begin{array}{ll} \beta = \dfrac{V_1}{\hbar\omega} & \mu = b\alpha \\[3ex] X = R\alpha & \gamma^2 = \dfrac{2m}{M} \\[3ex] \epsilon_0 = \dfrac{[p(j)]^2}{2m\hbar\omega} & \epsilon_1 = \dfrac{[p_1(f)]^2}{2m\hbar\omega} = \epsilon_0 + j - f \\[3ex] \epsilon_2 = \dfrac{[p_2(f)]^2}{2m\hbar\omega} = \epsilon_0 + j - f + \beta & h_0 = \gamma\epsilon_0^{1/2} \\[3ex] h_1 = \gamma(\epsilon_0 + j - f)^{1/2} & h_2 = \gamma(\epsilon_0 + j - f + \beta)^{1/2} \end{array}\right\} \tag{11}$$

As previously noted, because of the form of the general solution, the positive root is always chosen in calculating h_1 or h_2. For example, if for some f, $\epsilon_1 < 0$, h_1 is taken to be $i\gamma|\epsilon_1|^{1/2}$.

Using equation (4) and nondimensionalizing, equation (7) becomes

$$0 = \sum_{f=0}^{\infty} \psi_f(X)\left[C_f \exp(-ih_2 X) + D_f \exp(+ih_2 X)\right] \tag{12}$$

Some terms in equation (12) can be expanded in the complete orthonormal set of harmonic oscillator wave functions $\{\psi_n(X)\}$:

$$\exp(-ih_2 X)\psi_f(X) = \sum_{K=0}^{\infty} P_K(h_2, f)\psi_K(X) \tag{13}$$

$$\exp(+ih_2X)\psi_f(X) = \sum_{K=0}^{\infty} Q_K(h_2, f)\psi_K(X) \tag{14}$$

The matrix elements involved are readily available (ref. 7):

$$Q_K(h_2, f) = \left(\frac{f!K!}{2^{f+K}}\right)^{1/2} (ih_2)^{f+K} \exp\left[-\left(\frac{h_2}{2}\right)^2\right] \sum_{t=0}^{t_m} \frac{(-1)^t 2^t (h_2)^{-2t}}{t!(K-t)!(f-t)!} \tag{15}$$

where t_m is the smaller of the values f or K. When $+i$ is replaced by $-i$, $P_K(h_2, f)$ is identical to $Q_K(h_2, f)$. Substituting these expansions into equation (12) yields

$$0 = \sum_{K=0}^{\infty} \psi_K(X)\left[\sum_{f=0}^{\infty} C_f P_K(h_2, f) + D_f Q_K(h_2, f)\right] \tag{16}$$

Now, since $\{\psi_K(X)\}$ is complete and orthonormal, every coefficient of $\psi_K(X)$ in equation (16) must vanish:

$$0 = \sum_{f=0}^{\infty}\left[C_f P_K(h_2, f) + D_f Q_K(h_2, f)\right] \qquad K = 0, 1, \ldots, \infty \tag{17}$$

As shown in appendix C, the other three boundary conditions (eqs. (8) to (10)) can be treated similarly, yielding the following three sets of equations:

$$\sum_{f=0}^{\infty}\left\{A_j\delta_{fj} \exp(-ih_0\mu)\left[-S_K(h_0, j) + (2j)^{1/2}P_K(h_0, j-1)\right]\right.$$

$$+ B_f \exp(ih_1\mu)\left[-T_K(h_1, f) + (2f)^{1/2}Q_K(h_1, f-1)\right]$$

$$+ C_f \exp(-ih_2\mu)\left[S_K(h_2, f) - (2f)^{1/2}P_K(h_2, f-1)\right]$$

$$\left.+ D_f \exp(ih_2\mu)\left[T_K(h_2, f) - (2f)^{1/2}Q_K(h_2, f-1)\right]\right\} = 0 \qquad K = 0, 1, \ldots, \infty \tag{18}$$

8

$$\sum_{f=0}^{\infty} \left[-\delta_{fj}A_jh_0 \exp(-ih_0\mu)P_K(h_0,f) + B_fh_1 \exp(ih_1\mu)Q_K(h_1,f) \right.$$

$$\left. + C_fh_2 \exp(-ih_2\mu)P_K(h_2,f) - D_fh_2 \exp(ih_2\mu)Q_K(h_2,f) \right] = 0 \qquad K = 0, 1, \ldots \infty \qquad (19)$$

$$\sum_{f=0}^{\infty} \left[\delta_{fj}A_j \exp(-ih_0\mu)P_K(h_0,j) + B_f \exp(ih_1\mu)Q_K(h_1,f) \right.$$

$$\left. - C_f \exp(-ih_2\mu)P_K(h_2,f) - D_f \exp(ih_2\mu)Q_K(h_2,f) \right] = 0 \qquad K = 0, 1, \ldots \infty \qquad (20)$$

CALCULATION PROCEDURE

Numerical Approximation Technique

This fourfold infinite number of equations (eqs. (17) to (20)) in a threefold infinite number of unknowns (B_f, C_f, D_f, $f = 0, 1, \ldots \infty$) is approximated by a finite order matrix equation, which is then solved by computer. The f summation is taken only to some integer F, and K is cut off at some integer $\overline{K}$. Somewhat arbitrarily, each boundary condition is allowed to contribute equally to the approximating finite set by requiring that

$$3(F + 1) = 4(\overline{K} + 1) \qquad (21)$$

The left side of equation (21) gives the total number of unknowns in the finite set, while the right side gives the total number of equations in that set. Taking F and $\overline{K}$ high enough gives sufficiently converged values of $|B_f|^2$, $|C_f|^2$, and $|D_f|^2$, for small values of f. The computer program was written so that any positive integers F and $\overline{K}$ satisfying equation (21) could be used, thereby enabling the convergence of the answers of interest to be easily tested.

The input for the program is

ϵ_0 initial incoming particle energy, units of $\hbar\omega$

μ nondimensional rectangular well width

β nondimensional rectangular well depth

γ mass ratio

j   initial oscillator state

$F, \overline{K}$ cutoff indices

The output of the program included values of all the unknown coefficients B_0, B_1, ..., B_F, C_0, C_1, ..., C_F, D_0, D_1, ..., D_F separated into real and imaginary parts.

Current densities for the various component states were normalized by dividing them by the initial incoming density $[p(j)/m]|A_j|^2$, with $A_j = 1$. These normalized densities become (in terms of dimensionless units)

$$\left(\frac{\epsilon_0 + j - f + \beta}{\epsilon_0}\right)^{1/2} |C_f|^2$$

$$\left(\frac{\epsilon_0 + j - f + \beta}{\epsilon_0}\right)^{1/2} |D_f|^2$$

$$\left(\frac{\epsilon_0 + j - f}{\epsilon_0}\right)^{1/2} |B_f|^2$$

and are referred to as C_f-state densities, D_f-state densities, and B_f-state densities, respectively. For the cold-rare-gas-atom - cold-metallic-atom combinations of interest, ϵ_0, j, and β are all low, $\lesssim 3$ or 4. This leads to real, physically meaningful current densities only for low values of f, for which the squares of the coefficients $\left(|C_f|^2, \text{ etc.}\right)$ have accurately converged. When these densities were real, they were computed. Then, the normalized real C_f-state densities were summed, and this sum is defined as a C-state sum. Similarly, the appropriate D_f-state densities and B_f-state densities were summed. Convergence of these three sums was ensured by convergence of the individual densities.

Two other sums were formed by adding all normalized C_f-state densities, and then D_f-state densities, for which particle energy is less than zero but above the well bottom. These sums are referred to as bound-state sums.

Energy Accommodation Coefficient Calculation Procedure

The energy accommodation coefficient is defined as

$$\alpha_{ac} = \lim_{E_1 \to E_0} \left(\frac{E_0 - E_2}{E_0 - E_1}\right) \tag{22}$$

where E_0 is the mean energy of the incident particle, E_1 is the surface molecular energy, and E_2 is the average energy of particles leaving the surface. The definition is often stated in terms of corresponding temperatures, and is strictly accurate only if the temperature T_2 of particles leaving the surface is well defined. This is true if such particles have a Maxwellian velocity distribution. This distribution will be undistorted only when $T_0 \simeq T_1$ (ref. 12). The better experiments are conducted so that $\Delta T = T_0 - T_1$ (or $\Delta E = E_0 - E_1$) is as small as possible.

The computer results for the microscopic particle-oscillator interaction in the present model can be used to formulate theoretical values of α_{ac}. A microscopic energy accommodation coefficient is defined as

$$\alpha_j = \frac{E_{in} - E_{out}}{E_{in} - E_{osc}} \tag{23}$$

where

E_{in} incoming particle energy, $\epsilon_0 \hbar \omega$

E_{osc} energy of oscillator, $\left(j + \frac{1}{2}\right)\hbar\omega$

E_{out} average particle energy after interaction, calculated by weighting each of the possible stationary-state particle energies in the asymptotic region by calculated transition probabilities to these states, $\left[(\epsilon_0 + j - f)/\epsilon_0\right]^{1/2}|B_f|^2 = P_{j \to f}$, and then summing these weighted energies

This α_j is similar to Goodman's "effective a.c." of a single gas atom (ref. 11).

The surface is considered to be composed of independent oscillators, with the population of states given by the Boltzmann law

$$P(j) = \text{Fraction of oscillators in state } j$$

$$= \frac{\exp\left(-\dfrac{j\hbar\omega}{kT_s}\right)}{\displaystyle\sum_{j=0}^{\infty} \exp\left(-\dfrac{j\hbar\omega}{kT_s}\right)}$$

$$= \left[1 - \exp\left(-\frac{-\hbar\omega}{kT_s}\right)\right]\exp\left(-\frac{j\hbar\omega}{kT_s}\right) \tag{24}$$

where T_s is the effective surface temperature. If the incoming particle strikes the surface head on at a random oscillator, P(j) is also the probability that the particle strikes a j-state oscillator. Each oscillator is assumed to occupy the same fraction of surface area. This surface model is admittedly a poor one. For example, particles that miss the oscillators cannot be accounted for.

A thermally averaged accommodation coefficient $\overline{\alpha}_{calc}$ is defined by the equation

$$\overline{\alpha}_{calc} = \sum_{j=0}^{\infty} P(j)\alpha_j \tag{25}$$

In this equation, P(j) is regarded as constant in time by regarding the surface temperature T_s as being continually maintained by an external reservoir. A sample helium-tungsten calculation is given in appendix E, and the unimportance of states higher than j = 3 in equation (25) is shown.

Accuracy Checks

Several checks were made on the accuracy of the calculations. For the model of reference 2 (identical to the present model with zero well depth), Shuler and Zwanzig calculated probabilities of transitions in which the oscillator goes from state j to state f, while the incident particle momentum goes from $-p_j$ to $+p_f$. These probabilities, as in the present model, are given by

$$\left(\frac{\epsilon_0 + j - f}{\epsilon_0}\right)^{1/2} |B_f|^2 = P_{j \to f}$$

Their answers were duplicated when the well depth in the present model was set equal to zero, and $\gamma = 1.00$, for a range of well widths $0 < \mu \lesssim 100$. Computer results also indicate that with a depthless well, $\Psi_1(r, R) = \Psi_2(r, R)$, as far as the accurately calculated coefficients B_f, C_f, and D_f are concerned, as expected.

Microscopic reversibility (a result from energy conservation) holds in the present model in the form

$$P_{j \to f}\Big|_{\epsilon = \epsilon_0} = P_{f \to j}\Big|_{\epsilon = \epsilon_0 + j - f} \tag{26}$$

12

Conservation of current density provides checks on the B-, C-, and D-state sums defined previously. The total wave functions (eqs. (3) and (4)) can be used to show that the particle conservation requirement (total particle current density at any point must be zero) implies that the B-state sum must be equal to 1, and that the C- and D-state sums must be equal to each other.

The conventional form for current density is

$$\overline{S} = \frac{\hbar}{2im} (\Psi^* \nabla \Psi - \nabla \Psi^* \Psi) = \frac{\hbar}{m} \text{Im}(\Psi^* \nabla \Psi) \tag{27}$$

If particle motion without regard to the oscillator motion is of principal interest, the oscillator coordinate R in equation (27) is integrated out (ref. 13, pp. 126-128). Separability in the problem and normalization of the total wave functions with respect to R, but not r, make this the most straightforward procedure to follow to derive a relation satisfied by the coefficients. Setting the net particle current densities in the two regions equal to zero, one obtains

$$\overline{S}_1 = \frac{\hbar}{m} \int_{-\infty}^{\infty} \text{Im}\left[\Psi_1^*(r, R)\nabla_r \Psi_1(r, R)\right] dR = 0 \tag{28}$$

$$\overline{S}_2 = \frac{\hbar}{m} \int_{-\infty}^{\infty} \text{Im}\left[\Psi_2^*(r, R)\nabla_r \Psi_2(r, R)\right] dR = 0 \tag{29}$$

As shown in appendix D, equation (28) implies that the B-state sum must be equal to 1, and equation (29) implies only that the C- and D-state sums must be equal to each other. The common value of the C- and D-state sums may be less than, equal to, or greater than 1, depending on the input parameters. (The variance of these sums from 1 can be demonstrated analytically with a simplified version of the present model, having a potential like that in fig. 2 but fixed in space (e.g., R is set ≡ 0) with no energy exchange possible.) A physical explanation for this difference between incoming particle current density and that within the well is given in the RESULTS AND DISCUSSION section.

RESULTS AND DISCUSSION

Proposed Application to Trapping of a Gas Atom on the Surface of a Solid

Sticking probabilities are usually defined in experiments as fractions of incident gas atoms which are adsorbed on a surface, often by an expression of the form

$$\frac{\text{Incident beam intensity - Outcoming beam intensity}}{\text{Incident beam intensity}}$$

In many sticking probability experiments, the incident gas is not a beam, but just the part of a gas, injected into an evacuated chamber at a known rate, which strikes a known adsorbing surface. After the chamber pressure stabilizes, the adsorption rate on the surface must be just the flow rate into the chamber. Then, the sticking probability is just

$$\frac{\text{Rate of adsorption on surface}}{\text{Rate of collision with surface}}$$

where the denominator is calculated from kinetic theory.

In the present model, the total particle current density leaving the well equals the incoming density (the B-state sum equals 1). Thus, it is difficult to discuss trapping by using this definition of sticking probability.

However, in some classical models (e. g. , Goodman's in ref. 11), the sticking probability is taken as the fraction of gas particles which undergoes more than one collision with the surface, specifically, with a single surface layer atom. Recently (ref. 14), Goodman referred to such trapping as "apparent" trapping and stated that classical theories that use such a definition greatly overestimate the few reliable experimental measurements of trapping probabilities. However, he stated that "any one definition is probably not the most suitable for all purposes." These classical models allow energy to be exchanged between the oscillator-particle system and a one- or three-dimensional lattice during the interaction. This is not done in the present model. (Only in the energy accommodation coefficient calculation were oscillators permitted to be restored to their original states, and then only after the interaction.)

In a quantum-mechanical model, conditions cannot be determined for a gas particle definitely to undergo more than one collision with the surface. Nor can meaning be ascribed to a collision with the oscillator in a prescribed phase, or to an nth collision during the interaction. Although these restrictions are recognized, trapping in the present model can still be discussed from the standpoint of multiple collisions. It is suggested that probability current densities in the well may be interpreted physically in terms of multiple collisions. The conditions under which a gas particle is most likely to undergo more than one collision with the surface are determined, as shown when the results for helium and neon on tungsten are discussed.

Current densities calculated within the well are shown by Beder (ref. 15) to be close numerical approximations to actual physical mass fluxes in the various states, as would be observed in an ensemble of classical systems. He gives an involved analysis of mass fluxes in a potential similar to that of figure 2, but fixed in space (not fastened to a moving

oscillator). Briefly, he states that if the particle energy eigenfunction is approximately an expansion in particle momentum eigenfunctions for a limited region of space, this approximate expansion will furnish approximate relative particle number densities for the accessible momentum states, when measurements are taken anywhere in the limited region. In the present model, the particle energy eigenfunction is immediately an expansion in particle momentum eigenfunctions (plane waves) and hence will furnish meaningful particle densities.

Results for Helium and Neon on Tungsten

The input parameters for helium on tungsten are as follows:

$$\gamma = \left(\frac{2m}{M}\right)^{1/2} = 0.2087$$

$$\omega = 0.3 \frac{k\theta_D}{\hbar} \quad \text{(using appendix B of ref. 11)}$$

$$\omega = 1.31 \times 10^{13} \text{ sec}^{-1} \quad \text{for tungsten}$$

$$\left.\begin{array}{l} \beta = 0.7045 \\[1em] \mu = 20.76 \\[1em] \mu = 36.33 \end{array}\right\} \text{(see appendix B)}$$

The initial particle energy, in units of $\hbar\omega$, was varied from $\epsilon_0 = 0.025$ to 1.50 (with another calculation at $\epsilon_0 = 1.90$). For the approximate correlation $\frac{1}{2} kT \simeq \epsilon_0 \hbar\omega$, this ϵ_0 range corresponds to a gas temperature range of 5 to 300 K. (The mean kinetic energy of a one-dimensional Maxwellian beam is $\frac{1}{2} kT$ (ref. 2, p. 1783).) Temperature must be correlated with energy only for a one-dimensional beam to obey the principal of detailed balancing (ref. 2, p. 1783). This principal ensures thermal equilibrium in a statistical ensemble of particle-oscillator systems. The initial oscillator states chosen were j = 0, 1, and 2. As seen from appendix E, most surface atoms envisioned as oscillators at surface temperatures in the range from 5 to 300 K would be in these low states.

Table I gives the normalized, real probability current densities and the three density sums, for a typical set of input parameters shown in figure 3, for the helium-tungsten combination.
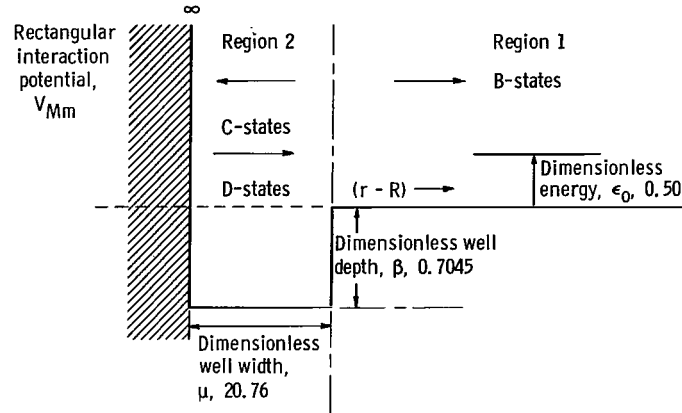
Figure 3. - The input parameters for a sample case of helium-tungsten combination. Mass ratio, γ, 0.2087; initial oscillator state, j, 1; fundamental frequency of oscillator, ω, 1.31×10^{13} per second. Current densities presented in table I.

TABLE I. - CURRENT DENSITIES AND DENSITY SUMS FOR SAMPLE CASE OF

HELIUM-TUNGSTEN COMBINATION

[Input parameters shown in fig. 3. Dimensionless energy, ϵ_0, 0.50; dimensionless well width, μ, 20.76; dimensionless well depth, β, 0.7045; mass ratio, γ, 0.2087; initial oscillator state, j, 1; fundamental frequency of oscillator, ω, 1.31×10^{13} sec^{-1}. C-state sum = D-state sum = 1.5519; B-state sum = 1.0000.]

Final oscillator energy level, f	Well current density		Transition probability,
	$\left(\dfrac{\epsilon_0 + j - f + \beta}{\epsilon_0}\right)^{1/2} |C_f|^2$	$\left(\dfrac{\epsilon_0 + j - f + \beta}{\epsilon_0}\right)^{1/2} |D_f|^2$	$\left(\dfrac{\epsilon_0 + j - f}{\epsilon_0}\right)^{1/2} |B_f|^2$
0	0.0095	0.1777	0.1831
1	1.3489	1.1787	.8169
2	.1935	.1955	Imaginary
3	Imaginary	Imaginary	Imaginary

If the initial incoming particle energy ϵ_0 is allowed to vary, the C- and D-state sums vary with ϵ_0, as shown in figures 4(a), (b), and (c) for j = 0, 1, and 2, respectively. Each figure gives results for the two well widths mentioned previously. As shown in appendix C, these sums need not be equal to 1, and a possible physical explanation for their variance from 1 is now offered.

Requiring the C- and D-state sums to be equal to 1 would apparently be requiring, in a physical sense, that the same number of particles be found moving to the right and to
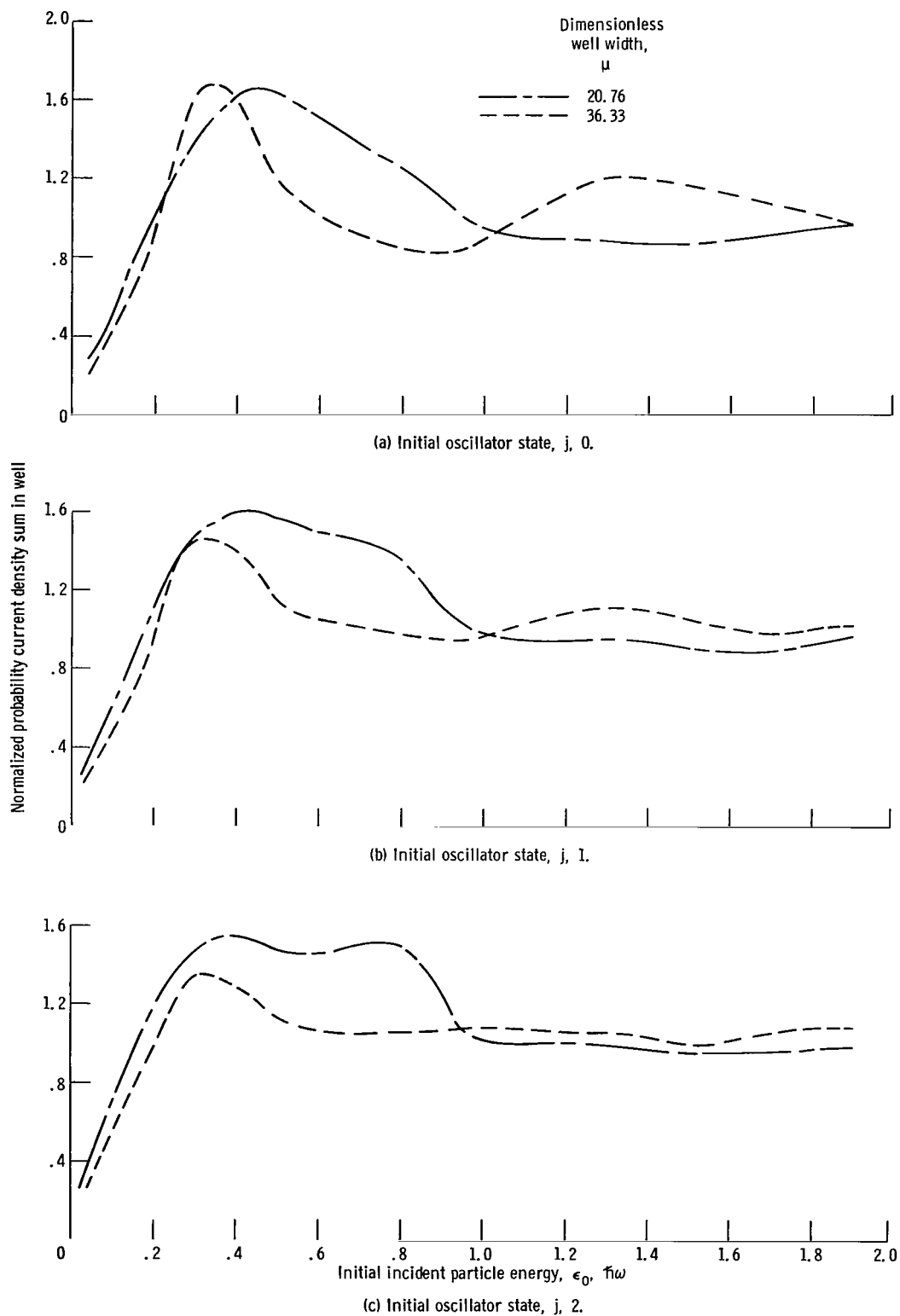
16

Figure 4. – Probability current density sum in well for helium-tungsten combination. Fundamental frequency of oscillator, ω, 1.31×10^{13} per second; mass ratio, γ, 0.2087; dimensionless well depth, β, 0.7045.

(a) Initial oscillator state, j, 0.

(b) Initial oscillator state, j, 1.

(c) Initial oscillator state, j, 2.

17

the left in the well region as are coming in toward the well from $+\infty$ with initial momentum p(j). However, both reflection and transmission can occur at the barrier $r - R = b$, regardless of particle energy or direction of impingement. Also, definite reflection is occurring at the other end of the well, the infinite wall. For certain choices of input parameters, all particles coming toward the well would not be expected to enter the well. In these cases, the C- and D-state sums, envisioned as "mass counters," would not "count" these particles at all and might be expected to be less than 1. Now, those particles that do enter the well region can suffer multiple collisions and accompanying changes of their energy. One interpretation is that these well sums may "count" some particles more than once. The same particle could conceivably contribute to current densities for various component states in $\Psi_2(r, R)$, associated with particle motion in the same direction (left or right), as the result of multiple collisions plus accompanying energy transfers. Therefore, the sums might be expected to be greater than 1. Only the complete mathematical solution can reveal which situation predominates for a given set of input parameters and whether the sums will be less than, equal to, or greater than 1.

However, for low incident particle energies, initial reflection from $r - R = b$ might be expected to predominate, as it does for a low energy particle impinging on a similar barrier fixed in space. Then, the well sums would be less than 1, and this is indicated in figure 4. Also, for high incident particle energies $(\epsilon_0 \gg \beta$, the well depth), the well sums might be expected to approach the value they would have if the well were not there; that is, 1, and this is indicated in figure 4.

Figure 4 shows that the current density sum in the well has a maximum value in the ϵ_0 interval $0.3 < \epsilon_0 < 0.5$. If this sum is a measure of the frequency of multiple collisions within the well, a helium atom with ϵ_0 in this interval has the best chance of being trapped, in the "apparent" sense of trapping.

Results show that neon-tungsten well sums have more local maximums over the ϵ_0 range of figure 4 than helium-tungsten well sums. And the magnitudes of these maximums are much greater for neon than for helium. For example, for the neon-tungsten combination, the following input parameters were chosen: $\gamma = 0.4686$, $\omega = 1.31 \times 10^{13}$ per second, $\beta = 3.17025$, $\mu = 20.76$, and $j = 0$. Again, the energy ϵ_0 was varied from 0.025 to 1.90, and well dimensions were based on Goodman's Morse potential data (ref. 11). The input for the corresponding helium-tungsten case was the same as for neon-tungsten, except with $\beta = 0.7045$ and $\gamma = 0.2087$.

The well density sum for neon-tungsten had about four local maximums in this ϵ_0 range (figure not shown). The values of these maximums varied from 3.1 to 9.2. The corresponding helium-tungsten case is presented in figure 4(a). This figure shows that the well sum for $\mu = 20.76$ has only one local maximum, which occurs at $\epsilon_0 \simeq 0.45$. Its value is about 1.65. The greater number of local maximums over a given ϵ_0 range and greater magnitudes of these local maximums for neon may suggest higher sticking

probabilities for neon than for helium on tungsten. Goodman also predicted this difference in sticking probabilities for helium and neon by using classical mechanics (ref. 11). Unfortunately, to our knowledge, experimental trapping data for monoenergetic helium and neon beams incident on tungsten does not exist.

Relative Magnitudes of C_f-State and D_f-State Densities

An interesting and, as yet, unexplained result occurs whenever the input parameters (for helium or neon on tungsten) are such that there exists only one possible stationary B_f state. This state is the same as the initial incoming state with the opposite sign for particle velocity; that is, the particle can only leave the well with an energy equal to its initial incoming energy. From energy considerations, this can happen only when $j = 0$ and $\epsilon_0 < 1$. When this occurs, not only are the C- and D-state sums equal, but also the individual corresponding C_f- and D_f-state densities are equal (to nearly eight-significant-place accuracy of the computer printout); that is,

$$\frac{\left[p_2(f)\right]}{m} |C_f|^2 = \frac{\left[p_2(f)\right]}{m} |D_f|^2$$

for all values of γ, μ, and β examined thus far. When ϵ_0 is varied to slightly above 1, and then two B_f states are possible (B_0 and B_1), this term-by-term equality is destroyed, but the C- and D-state sums are still equal.

The equality is destroyed in a somewhat predictable way, though. In the statistical interpretation, because of the direction of particle motion associated with C_f and D_f states, particles in C_f states could include some that have not "struck" the infinite wall, whereas all particles in D_f states have "struck" the infinite wall at least once. If most of the energy transfer occurs through collisions with the infinite wall, the set of C_f-state densities might be expected to indicate a higher probability of the initial state j than the D_f-state densities. Indeed, the C_j density is always larger than the D_j density, except in cases where the term-by-term equality mentioned previously holds (see e.g., table I).

Bound-State Sums

The bound-state sums defined previously were not extensively investigated. The physical phenomenon of sticking implies the presence of the gas particle near the surface, and it was believed that all states in the well (and their associated current densities) should be of interest - not just those corresponding to particle energies less than zero.

·A particle in the ell can be reflected at the barrier $r - R = b$ back toward the wall regardless of its total energy. Available results for the helium-tungsten combination indicate that these two bound-state sums are not, in general, equal, but that they increase with increasing well depth β, as might be expected.

Energy Accommodation Coefficient Results

The comparison between $\bar{\alpha}_{calc}$ and experimental data for α_{ac}, for helium on tungsten, is shown in figure 5. The experimental curve was drawn from data compiled from
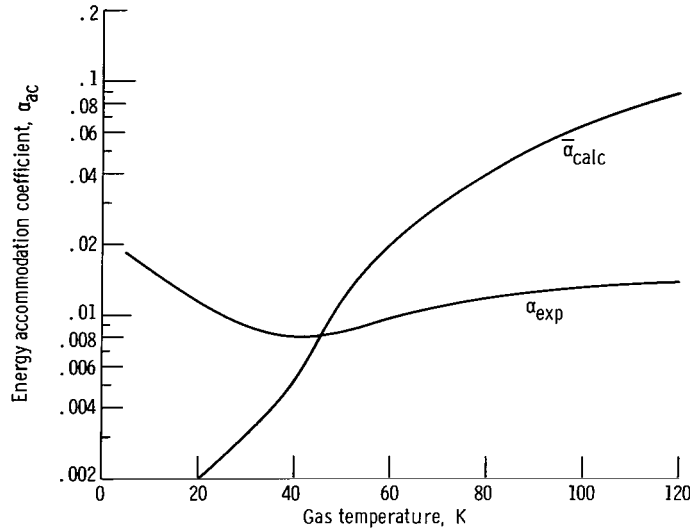
Figure 5. - Energy accommodation coefficient of helium on clean, cold tungsten. Experimental curve taken from data compiled by Trilling (ref. 16). Gas temperature assumed equal to wall temperature (see discussion following eq. (22)). Mass ratio, γ, 0.2087; fundamental frequency of oscillator, ω, 1.31×10^{13} per second; dimensionless well width, μ, 20.76; dimensionless well depth, β, 0.7045.

several sources (Silvernail, Thomas, Tho-Nhan, Wachman) and presented by Trilling (ref. 16). To enable a comparison between $\bar{\alpha}_{calc}$, for a monoenergetic gas beam and α_{exp} for a Maxwell-Boltzmann gas, the approximate correlation $\frac{1}{2} kT \simeq \epsilon_0 \hbar \omega$ was again made. (See the section Results for Helium and Neon on Tungsten). Note that none of the input parameters (in particular β and μ) were specially chosen to give the best agreement between $\bar{\alpha}_{calc}$ and $\bar{\alpha}_{exp}$.

For the temperature range from 20 to 120 K, the simple theory underestimates the accommodation coefficient at the lower temperatures and overestimates it at the higher

temperatures. In particular, the simple theory yields a limit of zero for $\overline{\alpha}_{calc}$, as the surface and gas temperatures approach zero. As the limit of zero temperature is approached, practically all the oscillators are in the ground state (j = 0). The gas particle approaches the oscillator with energy $\epsilon_0 \ll \hbar\omega$, and no phonons can be exchanged after the gas particle returns to $+\infty$ after interacting with an oscillator in state j = 0. Therefore, $E_{in} = E_{out}$ in equation (23), and $\alpha_j = \alpha_0 = 0$. Therefore, $\overline{\alpha}_{calc}$ approaches zero. Goodman's classical theory (ref. 11) has a low temperature limit of 1, and a minimum with varying temperature for helium-tungsten which is supported by recent experiments (fig. 5).

Goodman's theory yields a high temperature limit for the effective accommodation coefficient of a single gas atom of $4(m/M)/[1 + (m/M)]^2$, which equals 0.0833 for the helium-tungsten combination. This value seems to be exceeded by $\overline{\alpha}_{calc}$ at the higher temperatures of figure 5. However, it must be noted that this familiar classical hard sphere limit of $4(m/M)/[1 + (m/M)]^2$ is a limit only as the incident gas particle energy (temperature) approaches $+\infty$. The energy (temperature) of the solid atom is still taken as zero in this limit. On the other hand, the temperature of figure 5 is (approximately) both the surface and incident gas temperature, in accordance with the limit definition in equation (22). The high temperature limit of $\overline{\alpha}_{calc}$ in figure 5 has not been ascertained because the computer cannot calculate accurate transition probabilities (and hence E_{out} in eq. (23)) when ϵ_0 and j become large.

There are several possible reasons for the discrepancy in figure 5. Calculations were performed only for one fundamental frequency, where actually, a frequency spectrum (e.g., Debye) should be considered. The calculation of α_j could be repeated for many frequencies, and by weighting the results in accordance with the relative occurrence of those frequencies in the Debye spectrum, possibly a more accurate accommodation coefficient could be derived. Also, the calculation could be repeated for many incoming particle energies, and the results weighted in accordance with the relative occurrence of those energies in a one-dimensional Maxwell-Boltzmann energy distribution, to give a theoretically more accurate gas-temperature - gas-energy correlation. Such calculations have not as yet been performed because they require excessive computer time.

Furthermore, the trouble could be inherent in the model. Allowing the gas particles to make only direct, head-on, one-dimensional collisions with single surface layer particles, with no energy transfer to and from the neighboring lattice particles, could quite possibly yield misleading values for the accommodation coefficient. Also, the assumed interaction potential is a rather poor approximation to the more realistic Lennard-Jones or Morse potentials. Attempts to remedy most of these model deficiencies lead to a considerable increase in the complexity of a quantum-mechanical solution.

Since the calculation of $\overline{\alpha}_{calc}$ involves only the transition probabilities in the asymptotic region,

$$\left(\frac{\epsilon_0 + j - f}{\epsilon_0}\right)^{1/2} |B_f|^2 = P_{j \to f}$$

the importance of including the well in the model for a study of accommodation coefficients may be questioned. That the well presence significantly affects such probabilities, and hence $\bar{\alpha}_{calc}$, is shown in table II. In each of the two sample cases ($\epsilon_0 = 0.400$ and $\epsilon_0 = 1.500$), the probability that the oscillator is found in its initial state (j = f = 1) when the particle is approaching $+\infty$ after the interaction is definitely smaller when the well is present than with no well at all.

TABLE II. - EFFECT OF WELL PRESENCE ON TRANSITION

PROBABILITIES FOR HELIUM ON TUNGSTEN

[Mass ratio, γ, 0.2087; dimensionless well width, μ, 20.76; initial oscillator state, j, 1.]

Final oscillator energy level, f	Dimensionless well depth, β	Initial energy of particle, ϵ_0	Transition probability, $\left(\dfrac{\epsilon_0 + j - f}{\epsilon_0}\right)^{1/2} |B_f|^2$
0	0	0.400	0.0628
1	0		.9372
2	0		Imaginary
0	.07045		0.1703
1	.07045		.8297
2	.07045		Imaginary
0	0	1.500	0.1502
1	0		.7156
2	0		.1342
3	0		Imaginary
0	.07045		0.1649
1	.07045		.5254
2	.07045		.3097
3	.07045		Imaginary

SUMMARY OF RESULTS

The Schrödinger equation was solved numerically for a one-dimensional collision between a harmonic oscillator and a particle with a rectangular trapping potential. General solutions were sums of states, each a product of a particle wave function and an oscillator wave function.

A correlation was suggested between probability current densities for states within the well and sticking of gas atoms on surfaces, where sticking is regarded as arising from multiple collisions. Energy accommodation coefficients were formulated and compared with helium-tungsten experiments for the temperature range 20 to 120 K. The theory underestimates the accommodation coefficient at lower temperatures and overestimates it at higher temperatures. Results indicate that only approximate qualitative predictions of the coefficient are possible with this simplified model.

Lewis Research Center,
National Aeronautics and Space Administration,
Cleveland, Ohio, September 11, 1968,
124-09-19-01-22.

APPENDIX A

SYMBOLS

A_j, B_f, C_f, D_f coefficients in $\Psi_1(r, R)$ and $\Psi_2(r, R)$

a   constant in Morse potential, $\mathring{A}^{-1}$; m^{-1}

b   well width, m

D   constant in Morse potential, kcal/mole; J/mole

E_{in} initial particle energy, $\epsilon_0 \hbar\omega$, J

E_{osc} harmonic oscillator energy, $\left(n + \frac{1}{2}\right)\hbar\omega$; n = 0, 1, ... ∞, J

E_{out} average outcoming particle energy, calculated in text and appendix E, J

E_0 average energy of incident particle in definition of α_{ac}, J

E_1 average surface molecular energy, in definition of α_{ac}, J

E_2 average energy of gas particles leaving surface, in definition of α_{ac}, J

E(1), E(2)   Schrödinger equation energies for regions 1 and 2, respectively, J

$F, \overline{K}$ cutoff indices

$\mathscr{F}_1$ largest value of f for which $\left[p_1(f)\right]$ is real

$\mathscr{F}_2$ largest value of f for which $\left[p_2(f)\right]$ is real

$H_n(\alpha R)$ Hermite polynomial

$\hbar$ $h/2\pi$, where h = Planck's constant = 6.6256×10^{-34} J-sec

h_0 derived quantity, $\gamma \epsilon_0^{1/2}$

h_1 derived quantity, $\gamma(\epsilon_0 + j - f)^{1/2}$

h_2 derived quantity, $\gamma(\epsilon_0 + j - f + \beta)^{1/2}$

j, f   positive integers denoting initial and final oscillator states, respectively, 0, 1, ... ∞

K   summation index

k   Boltzmann constant, 1.38054×10^{-23} J/K

M   mass of oscillator, kg

m   mass of particle, kg

P(j)   fraction of oscillators in state j, from Boltzmann distribution, $\exp\left(-\dfrac{j\hbar\omega}{kT_s}\right)\left[1 - \exp\left(\dfrac{-\hbar\omega}{kT_s}\right)\right]$

$P_{j \to f}$ oscillator transition probability, $\left(\dfrac{\epsilon_0 + j - f}{\epsilon_0}\right)^{1/2} |B_f|^2$

24

$P_K(h_l, f)$	expansion coefficient, defined in text, $l = 0, 1, 2$	$\bar{S}_1, \bar{S}_2$	total particle current densities in regions 1 and 2, respectively
$p(j)$	initial particle momentum, (kg)(m)/sec	T	temperature, K
$p_1(f)$	particle momentum, in region 1 when oscillator is in state f, (kg)(m)/sec	$T_K(h_l, f)$	expansion coefficient, defined in appendix C, $l = 0, 1, 2$
$[p_1(f)]$	denotes choice of positive root, real or imaginary, when $p_1(f)$ is calculated from eq. (5)	T_s	surface temperature, K
		T_0	temperature of incident particles, in definition of α_{ac}, K
$p_2(f)$	particle momentum, in region 2, when oscillator is in state f, (kg)(m)/sec	T_1	temperature of surface molecules in definition of α_{ac}, K
$[p_2(f)]$	denotes choice of positive root, real or imaginary, when $p_2(f)$ is calculated from eq. (6)	T_2	temperature of gas particles leaving surface, in definition of α_{ac}, K
$Q_K(h_l, f)$	expansion coefficient, defined in text, $l = 0, 1, 2$	V_{Mm}	rectangular interaction potential, J
R	coordinate of oscillator, Å; m	V_1	well depth in V_{Mm}, J
r	reduced particle coordinate, $r' - X_0 + \dfrac{\ln 2}{a}$, Å; m	$v(r' - R)$	Morse potential, $D\left\{\exp\left[-2a(r' - R - X_0)\right] - 2\exp\left[-a(r' - R - X_0)\right]\right\}$, kcal/mole; J/mole
r'	coordinate of particle, Å; m	X	dimensionless coordinate of oscillator, αR
∇_r	gradient operator with respect to r	X_0	equilibrium separation in Morse potential, Å; m
r_o	nominal radius of oscillator, m	x	dimensionless reduced particle coordinate, αr
r_p	nominal radius of particle, m	α	reciprocal of characteristic harmonic oscillator length, $(M\omega/\hbar)^{1/2}$, m^{-1}
$\bar{S}$	total current density		
$S_K(h_l, f)$	expansion coefficient, defined in appendix C, $l = 0, 1, 2$	α_{ac}	energy accommodation coefficient, $\lim\limits_{E_1 \to E_0}\left(\dfrac{E_0 - E_2}{E_0 - E_1}\right)$

$\bar{\alpha}_{calc}$ thermal average of α_j values, $\sum\limits_{j=0}^{\infty} P(j)\alpha_j$

α_{exp} experimental value of $\alpha_{ac.}$ for helium on tungsten, taken from data compiled by Trilling (ref. 16)

α_j microscopic energy accommodation coefficient, $(E_{in} - E_{out})/(E_{in} - E_{osc})$

β dimensionless well depth, $V_1/\hbar\omega$

γ mass ratio, $(2m/M)^{1/2}$

δ_{fj} Kronecker delta: 1, if $f = j$; 0, if $f \neq j$

ϵ_0 dimensionless energy, $[p(j)]^2/2m\hbar\omega$

ϵ_1 dimensionless energy, $[p_1(f)]^2/2m\hbar\omega$

ϵ_2 dimensionless energy, $[p_2(f)]^2/2m\hbar\omega$

θ_D Debye temperature, K

μ dimensionless well width, αb

ξ_n normalization constant in $\psi_n(r)$, $[\alpha/(\pi^{1/2}2^n n!)]^{1/2}$

$\Psi_1(r, R)$, $\Psi_2(r, R)$ Schrödinger equation solutions for regions 1 and 2, respectively

$\psi_n(R)$ harmonic oscillator wave function, $\xi_n \exp\left(-\tfrac{1}{2}\alpha^2 R^2\right) H_n(\alpha R)$; $n = 0, 1, \ldots \infty$

ω fundamental frequency of oscillator, $\sec^{-1}$

APPENDIX B

RELATION BETWEEN MORSE AND RECTANGULAR WELL POTENTIALS

Equilibrium occurs in the Morse potential when the coordinates of the oscillator and particle are separated by the distance X_0; that is, when $r' - R = X_0$. Then, the Morse potential (fig. 6) can be written as

$$v(r' - R) = D\left\{\exp\left[-2a(r' - R - X_0)\right] - 2\exp\left[-a(r' - R - X_0)\right]\right\} \tag{B1}$$

The parameter D is the depth of the Morse potential well, and the reciprocal of the parameter a is a measure of the width of the well.

A rectangular well, with one side as an infinite wall, will be used to approximate the Morse potential. During development of this approximation, for convenience in subsequent calculations, a new coordinate r, linearly related to r', will be introduced.

The coordinate of the infinite potential wall on the $(r' - R)$ scale of figure 6 will be fixed arbitrarily at

$$(r' - R)_{wall} = X_0 - \frac{\ln 2}{a} \tag{B2}$$

If a new coordinate is defined

$$r \equiv r' - X_0 + \frac{\ln 2}{a}$$

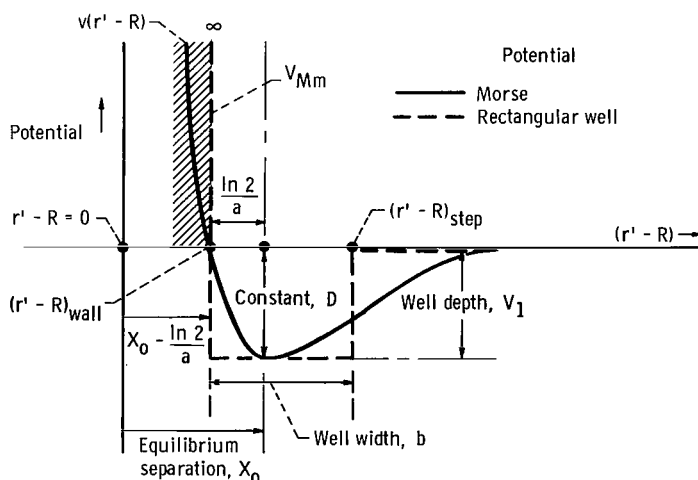
Figure 6. – Morse potential $v(r' - R)$ and rectangular well potential V_{Mm}.

equation (B2) can be written as

$$\left(r' - R - X_0 + \frac{\ln 2}{a}\right)_{\text{wall}} = (r - R)_{\text{wall}} = 0 \tag{B3}$$

The other end of the rectangular well, the potential step, will be fixed at

$$(r' - R)_{\text{step}} = X_0 - \frac{\ln 2}{a} + b \tag{B4}$$

where b is the rectangular well width (see fig. 6). Again, using the coordinate r gives equation (B4) in the form

$$\left(r' - R - X_0 + \frac{\ln 2}{a}\right)_{\text{step}} = (r - R)_{\text{step}} = b \tag{B5}$$

The transformation to coordinates r and R is not absolutely necessary. The algebraic form of some subsequent equations is slightly simpler if one end of the rectangular well occurs at a point where the difference of the coordinates chosen is zero $(r - R)_{\text{wall}} = 0$. Thus, the interaction potential V_{Mm} becomes that shown in figure 2.

For this initial study, one value of well depth $V_1 = D$ was chosen, and the well width b was treated as a variable parameter. For the helium-tungsten combination, two values of b were arbitrarily chosen, $b = (2 \ln 2)/a$ and $b = (3.5 \ln 2)/a$. Using Goodman's values of $a = 1.3$ per angstrom and $D = 0.14$ kilocalorie per mole (5.86×10^2 J/mole) for this combination (ref. 11), $\omega = 1.31\times10^{13}$ per second (using appendix B of ref. 11), and equation (11), gives the well depth β as 0.7045 and the two well widths as $\mu = 20.76$ and 36.33, respectively.

APPENDIX C

REDUCTION OF BOUNDARY-CONDITION EQUATIONS

Consider equation (8). The normalized oscillator wave functions are given by

$$\psi_n(X) = \xi_n \exp\left(-\frac{1}{2}X^2\right)H_n(X) \qquad X = \alpha R \qquad (C1)$$

where

$$\xi_n = \left(\frac{\alpha}{\pi^{1/2}2^n n!}\right)^{1/2}$$

and

$$\int_{-\infty}^{\infty} |\psi_n(X)|^2 \, dX = \alpha$$

Using the relation $(d/dX)H_n(X) = 2nH_{n-1}(X)$, one can show that

$$\frac{d}{dR}\psi_n(R) = \left[\frac{d}{dX}\psi_n(X)\right]\frac{dX}{dR} = \alpha \, \xi_n \exp\left(-\frac{X^2}{2}\right)\left[-XH_n(X) + 2nH_{n-1}(X)\right] \qquad (C2)$$

Substituting equations (3) and (4) into equation (8) and using equations (11) and (C2) yield the following equation:

$$A_j \exp\left[-ih_0(X + \mu)\right]\alpha \, \xi_j \exp\left(-\frac{X^2}{2}\right)\left[-XH_j(X) + 2jH_{j-1}(X)\right]$$

$$+ \sum_{f=0}^{\infty} B_f \exp\left[+ih_1(X + \mu)\right]\alpha \, \xi_f\left[-XH_f(X) + 2fH_{f-1}(X)\right]\exp\left(-\frac{X^2}{2}\right) = \sum_{f=0}^{\infty} \left\{C_f \exp\left[-ih_2(X + \mu)\right]\right.$$

$$\left. + D_f \exp\left[+ih_2(X + \mu)\right]\right\}\alpha \, \xi_f \exp\left(-\frac{X^2}{2}\right)\left[-XH_f(X) + 2fH_{f-1}(X)\right] \qquad (C3)$$

Now consider the combination of the form $\xi_j j H_{j-1}(X)$ in equation (C3). From the definition of ξ_n, it is apparent that

$$\xi_{j-1} = \left[\frac{\alpha}{\pi^{1/2} 2^{j-1} (j-1)!} \right]^{1/2} = (2j)^{1/2} \xi_j \qquad \text{(C4a)}$$

or

$$\xi_j = (2j)^{-1/2} \xi_{j-1} \qquad \text{(C4b)}$$

Therefore,

$$A_j \exp\left[-ih_0(X+\mu)\right] \alpha \exp\left(-\frac{X^2}{2}\right) (2j)^{-1/2}(2j)\xi_{j-1} H_{j-1}(X)$$

$$= A_j \exp\left[-ih_0(X+\mu)\right] \alpha (2j)^{1/2} \psi_{j-1}(X) \qquad \text{(C5)}$$

Using equations (C4) and (C5), with the possible substitution of f for j in equations (C4), reduces equation (C3) to

$$A_j \exp\left[-ih_0(X+\mu)\right]\left[-\alpha X\psi_j(X) + \alpha(2j)^{1/2}\psi_{j-1}(X)\right]$$

$$+ \sum_{f=0}^{\infty} B_f \exp\left[+ih_1(X+\mu)\right]\left[-\alpha X\psi_f(X) + (2f)^{1/2}\alpha\psi_{f-1}(X)\right] = \sum_{f=0}^{\infty}\left\{ C_f \exp\left[-ih_2(X+\mu)\right] \right.$$

$$\left. + D_f \exp\left[+ih_2(X+\mu)\right]\right\}\left[-\alpha X\psi_f(X) + (2f)^{1/2}\alpha\psi_{f-1}(X)\right] \qquad \text{(C6)}$$

Some terms in equation (C6) are expanded as follows:

$$\exp(+ih_l X)X \, \psi_f(X) = \sum_{K=0}^{\infty} T_K(h_l, f)\psi_K(X) \qquad \text{(C7)}$$

where $l = 0$, 1, or 2, and

$$\alpha T_K(h_l, f) = \int_{-\infty}^{\infty} \exp(ih_l X)X\psi_f(X)\psi_K(X)dX$$

$$= \left(\frac{1}{i}\right)\frac{\partial}{\partial h_l}\left[\alpha Q_K(h_l, f)\right] \qquad \text{(C8)}$$

30

Using equations (C8) and (15) shows, after some rearrangement, that

$$T_K(h_l, f) = \left(\frac{f! K!}{2^{f+K}}\right)^{1/2} \exp\left[-\left(\frac{h_l}{2}\right)^2\right] h_l^{f+K} \left(i^{f+K+1}\right) \left[\left(\frac{h_l}{2} - \frac{f+K}{h_l}\right) \sum_{t=0}^{t_m} \frac{(-1)^t 2^t (h_l)^{-2t}}{t!(K-t)!(f-t)!}\right.$$

$$\left. - \sum_{t=0}^{t_m} \frac{(-1)^{t+1} 2^{t+1} t (h_l)^{-2t-1}}{t!(K-t)!(f-t)!}\right] \tag{C9}$$

where $l = 0$, 1, or 2, and t_m is the smaller of the values f or K. Some terms in equation (C6) are also expanded as follows:

$$\exp(-ih_l X) X \psi_f(X) = \sum_{K=0}^{\infty} S_K(h_l, f) \psi_K(X) \tag{C10}$$

with $S_K(h_l, f)$ having the same algebraic form as $T_K(h_l, f)$, with $+i$ replaced by $-i$.

Now, using equations (C7), (C10), (13), and (14) gives equation (C6), after interchanging orders of summation and letting

$$\delta_{fj} = \begin{cases} 1 & \text{if } f = j \\ 0 & \text{if } f \neq j \end{cases}$$

in the form:

$$\sum_{K=0}^{\infty} \psi_K(X) \left\{ \sum_{f=0}^{\infty} A_j \delta_{fj} \left[\exp(-ih_0 \mu) S_K(h_0, j) + (2j)^{1/2} P_K(h_0, j-1) \exp(-ih_0 \mu)\right]\right.$$

$$+ \sum_{f=0}^{\infty} B_f \exp(ih_1 \mu) \left[-T_K(h_1, f) + (2f)^{1/2} Q_K(h_1, f-1)\right]$$

$$+ \sum_{f=0}^{\infty} C_f \exp(-ih_2 \mu) \left[S_K(h_2, f) - (2f)^{1/2} P_K(h_2, f-1)\right]$$

$$\left. + \sum_{f=0}^{\infty} D_f \exp(ih_2 \mu) \left[T_K(h_2, f) - (2f)^{1/2} Q_K(h_2, f-1)\right]\right\} = 0 \tag{C11}$$

Now, once again, the completeness of the set $\left\{\psi_K(X)\right\}$ immediately yields equation (18) from equation (C11). A similar procedure leads from equation (9) to equation (19), and from equation (10) to equation (20); no new expansion coefficients are involved.

Because of the presence of h_l in some denominators in the algebraic forms of the expansion coefficients, the computer cannot evaluate the coefficients in these forms when $h_l = 0$. It is easiest then to return to the original definitions of the coefficients and to use the following equations, when $h_l = 0$ (ref. 17):

$$
\left.
\begin{aligned}
T_K(0, f) = S_K(0, f) &= \frac{1}{\alpha} \int_{-\infty}^{\infty} \psi_f^*(X) X \psi_K(X) dX \\[2ex]
&= \left(\frac{f + 1}{2}\right)^{1/2} \quad \text{if } K = f + 1 \\[2ex]
&= \left(\frac{f}{2}\right)^{1/2} \quad \text{if } K = f - 1 \\[2ex]
&= 0 \quad \text{Otherwise}
\end{aligned}
\right\} \tag{C12}
$$

$$
\left.
\begin{aligned}
Q_K(0, f) = P_K(0, f) &= \frac{1}{\alpha} \int_{-\infty}^{\infty} \psi_f^*(X) \psi_K(X) dX \\[2ex]
&= 1 \quad \text{if } K = f \\[2ex]
&= 0 \quad \text{Otherwise}
\end{aligned}
\right\} \tag{C13}
$$

TOTAL CURRENT DENSITY CALCULATIONS FOR REGIONS 1 AND 2

Using $\Psi_1(r, R)$ as given in equation (3) shows that

$$\Psi_1^* \nabla_r \Psi_1 = \left(A_j^* \psi_j(R) \exp\left\{ + \frac{i[p(j)]}{\hbar} \right\} \right.$$

$$+ \sum_{f=0}^{\infty} B_f^* \psi_f(R) \exp\left\{ - \frac{i[p_1(f)]^* r}{\hbar} \right\} \right) \left(A_j \psi_j(R) \left\{ - \frac{i[p(j)]}{\hbar} \right\} \exp\left\{ - \frac{i[p(j)]}{\hbar} \right\} \right.$$

$$\left. + \sum_{f=0}^{\infty} B_f \psi_f(R) \left\{ + \frac{i[p_1(f)]r}{\hbar} \right\} \exp\left\{ \frac{i[p_1(f)]r}{\hbar} \right\} \right) \tag{D1}$$

Note that $[p_1(f)]$ is now either real or pure imaginary, so that its complex conjugate is not, in general, equal to itself. Using equation (D1) and the orthonormality of the set $\{\psi_f(R)\}$ in equation (28), yields

$$\bar{S}_1 = 0 = \frac{\hbar}{m} \text{Im} \left(|A_j|^2 \left\{ - \frac{i[p(j)]}{\hbar} \right\} + A_j^* B_j \left\{ \frac{i[p(j)]}{\hbar} \right\} \exp\left\{ \frac{i2[p(j)]}{\hbar} \right\} \right.$$

$$\left. + B_j^* A_j \left\{ - \frac{i[p(j)]}{\hbar} \right\} \exp\left\{ - \frac{2i[p(j)]}{\hbar} \right\} + \sum_{f=0}^{\infty} |B_f|^2 \left\{ \frac{i[p_1(f)]}{\hbar} \right\} \exp\left\{ - \frac{i[p_1(f)]^* r}{\hbar} + \frac{i[p_1(f)]r}{\hbar} \right\} \right) \tag{D2}$$

If r is taken large enough, the last exponential in equation (D2)

$$\exp\left\{ \frac{-i[p_1(f)]^* r}{\hbar} + \frac{i[p_1(f)]r}{\hbar} \right\}$$

will be equal to 1 if $[p_1(f)]$ is real and will approach zero if $p_1(f) = i|p_1(f)|$. Doing this and noting that the third term in equation (D2) is simply the complex conjugate of the second term result in

$$\overline{S}_1 = 0 = \frac{-|A_j|^2[p(j)]}{m} + \sum_{f=0}^{\mathscr{F}_1} \frac{|B_f|^2[p_1(f)]}{m} \tag{D3}$$

where $\mathscr{F}_1$ is the greatest value of f for which $[p_1(f)]$ is real. Equation (D3) means that the B-state sum must equal 1.

Using $\Psi_2(r, R)$ as given in equation (4) and the orthonormality of the set $\{\psi_f(R)\}$ in equation (29) yields

$$\overline{S}_2 = 0 = \frac{\hbar}{m} \operatorname{Im} \left[\sum_{f=0}^{\infty} \left(|C_f|^2 \left\{ -\frac{i[p_2(f)]}{\hbar} \right\} \exp\left\{ +\frac{i[p_2(f)]^*r}{\hbar} \right\} \exp\left\{ -\frac{i[p_2(f)]r}{\hbar} \right\} \right. \right.$$

$$+ D_f^* C_f \left\{ -\frac{i[p_2(f)]}{\hbar} \right\} \exp\left\{ -\frac{i[p_2(f)]^*r}{\hbar} \right\} \exp\left\{ -\frac{i[p_2(f)]r}{\hbar} \right\}$$

$$+ C_f^* D_f \left\{ \frac{i[p_2(f)]}{\hbar} \right\} \exp\left\{ \frac{i[p_2(f)]^*r}{\hbar} \right\} \exp\left\{ \frac{i[p_2(f)]r}{\hbar} \right\}$$

$$\left. \left. + |D_f|^2 \left\{ \frac{i[p_2(f)]}{\hbar} \right\} \exp\left\{ -\frac{i[p_2(f)]^*r}{\hbar} \right\} \exp\left\{ \frac{i[p_2(f)]r}{\hbar} \right\} \right) \right] \tag{D4}$$

Next, the infinite sum is broken up and $\mathscr{F}_2$ is introduced as the greatest value of f for which $[p_2(f)]$ is real:

$$\overline{S}_2 = 0 = \frac{\hbar}{m} \operatorname{Im} \left[\sum_{f=0}^{\mathscr{F}_2} \left(|C_f|^2 \left\{ -\frac{i[p_2(f)]}{\hbar} \right\} + |D_f|^2 \left\{ \frac{i[p_2(f)]}{\hbar} \right\} \right) \right.$$

$$+ \sum_{f=\mathscr{F}_2+1}^{\infty} \left\{ |C_f|^2 \left[+\frac{|p_2(f)|}{\hbar} \right] \exp\left[+\frac{2|p_2(f)|r}{\hbar} \right] + D_f^* C_f \left[+\frac{|p_2(f)|}{\hbar} \right] + C_f^* D_f \left[-\frac{|p_2(f)|}{\hbar} \right] \right.$$

$$\left. \left. + |D_f|^2 \left[\frac{-|p_2(f)|}{\hbar} \right] \exp\left[-\frac{2|p_2(f)|r}{\hbar} \right] \right\} \right] = \sum_{f=0}^{\mathscr{F}_2} \left(|C_f|^2 \left\{ -\frac{[p_2(f)]}{m} \right\} + |D_f|^2 \left\{ \frac{[p_2(f)]}{m} \right\} \right) \tag{D5}$$

34

Equation (D5) implies that the C- and D-state sums must be equal, but nothing is said in equation (D5) about the magnitude of their common value. This value is a complicated function of the input parameters A_j, ϵ_0, j, γ, β, and μ.

APPENDIX E

SAMPLE CALCULATION FOR ENERGY ACCOMMODATION COEFFICIENT

The helium-tungsten combination is considered once again with $\gamma = 0.2087$, $\omega = 1.31\times10^{13}$ per second, $\mu = 20.76$, $\beta = 0.7045$, and $\epsilon_0 = 0.225$, corresponding to a gas temperature of approximately 45 K. This temperature was the apparent crossover point of theoretical and experimental curves for α_{ac} (see fig. 5). The surface temperature T_s will be assumed to be 45 K also. A difference of a few degrees would only slightly repopulate the surface layer oscillators.

For $j = 0$:

$$P_{0\to0} = 1.000$$

All other transitions are energetically impossible in the asymptotic region. Therefore,

$$E_{in} = 0.225\ \hbar\omega$$

$$E_{osc} = \left(0 + \frac{1}{2}\right)\hbar\omega$$

$$E_{out} = (1.0000)(0.225)\hbar\omega$$

$$\alpha_0 = \frac{E_{in} - E_{out}}{E_{in} - E_{osc}} = 0.0$$

For $j = 1$:

$$P_{1\to0} = 0.0930$$

$$P_{1\to1} = 0.9070$$

Dropping the $\hbar\omega$ yields

$$E_{in} = 0.225$$

$$E_{osc} = 1 + \frac{1}{2} = 1.500$$

$$E_{out} = (0.9070)(0.225) + (0.0930)(1.225)$$

$$\simeq 0.318$$

Note that if the oscillator went from $j = 1$ to $f = 0$, the particle energy must have changed from 0.225 to 1.225, so that 1.225 is weighted by $P_{1 \to 0}$ in E_{out}:

$$\alpha_1 = \frac{0.225 - 0.318}{0.225 - 1.5}$$

$$\simeq 0.0730$$

For $j = 2$:

$$P_{2 \to 0} = 0.0110$$

$$P_{2 \to 1} = 0.1900$$

$$P_{2 \to 2} = 0.7991$$

$$E_{in} = 0.225$$

$$E_{osc} = 2.5$$

$$E_{out} = (0.7991)(0.225) + (0.1900)(1.225) + (0.0110)(2.225)$$

$$\simeq 0.437$$

Therefore,

$$\alpha_2 = 0.0931$$

For $j = 3$:

$$P_{3 \to 0} = 0.0010$$

$$P_{3 \to 1} = 0.0335$$

$$P_{3 \to 2} = 0.2843$$

$$P_{3 \to 3} = 0.6812$$

$$E_{in} = 0.225$$

$$E_{osc} = 3.5$$

$$E_{out} = (0.6812)(0.225) + (0.2843)(1.225) + (0.0335)(2.225) + (0.0010)(3.225)$$

$$\simeq 0.5791$$

Therefore,

$$\alpha_3 = 0.1080$$

Now, with $T_s \simeq 45 \text{ K}$ and $\theta = \hbar\omega/k \simeq 100 \text{ K}$,

$$P(j) = \left(1 - e^{-\theta/T_s}\right)\left(e^{-j\theta/T_s}\right)$$

$$\cong (0.892)(0.1080)^j$$

$$P(0) \simeq 0.892$$

$$P(1) \simeq 0.0962$$

$$P(2) \simeq 0.0104$$

$$P(3) \simeq 0.001122$$

Therefore,

$$\bar{\alpha}_{calc} \simeq \sum_{j=0}^{3} P(j)\alpha_j \simeq 0.00812$$

The relative smallness of $P(j)\alpha_j$, for $j = 3$ and higher, makes possible summing to about $j = 3$ in the expression for $\bar{\alpha}_{calc}$. This holds true for the entire temperature range of figure 5.

REFERENCES

1. Chambre, P. L.; and Schaaf, S. A.: Flow of Rarefied Gases. Princeton Univ. Press, 1961.

2. Shuler, Kurt E.; and Zwanzig, Robert: Quantum-Mechanical Calculation of Harmonic Oscillator Transition Probabilities in a One-Dimensional Impulsive Collision. J. Chem. Phys., vol. 33, no. 6, Dec. 1960, pp. 1778-1784.

3. Devonshire, A. F.: The Interaction of Atoms and Molecules with Solid Surfaces. VIII - The Exchange of Energy Between a Gas and a Solid. Proc. Roy. Soc. (London), Ser. A, vol. 158, no. 894, Jan. 15, 1937, pp. 269-279.

4. Gilbey, D. M.: A Simple Model for Gas-Solid Energy Exchange. Rarefied Gas Dynamics. Vol. 1. C. L. Brundin, ed., Academic Press, Inc., 1967, pp. 101-108.

5. Secrest, Don; and Johnson, B. Robert: Exact Quantum-Mechanical Calculation of a Collinear Collision of a Particle with a Harmonic Oscillator. J. Chem. Phys., vol. 45, no. 12, Dec. 15, 1966, pp. 4556-4570.

6. Jackson, J. M.; and Mott, N. F.: Energy Exchange Between Inert Gas Atoms and a Solid Surface. Proc. Roy. Soc. (London), Ser. A, vol. 137, no. 833, Sept. 1, 1932, pp. 703-717.

7. Castellan, Gilbert W.; and Hulburt, Hugh M.: The Interchange of Translational and Vibrational Energy in an Asymmetric Molecular Potential Field. J. Chem. Phys., vol. 18, no. 3, Mar. 1950, pp. 312-322.

8. Widom, B.: One-Dimensional Inelastic Collisions with Impulsive Interactions. J. Chem. Phys., vol. 30, no. 1, Jan. 1959, pp. 238-245.

9. Diestler, Dennis J.; and McKoy, Vincent: Quantum-Mechanical Treatment of Inelastic Collisions. I. General Theory and Application to Nonreactive Collisions. J. Chem. Phys., vol. 48, no. 7, Apr. 1, 1968, pp. 2941-2950.

10. Sugawara, Motoaki: A Quantum Mechanical Theory of Adsorption of Inert Gas Atoms on a Solid Surface. NASA TT F-11493, 1968.

11. Goodman, F. O.: On the Theory of Accommodation Coefficients. V. Classical Theory of Thermal Accommodation and Trapping. Rarefied Gas Dynamics. Vol. 2. J. H. deLeeuw, ed., Academic Press, Inc., 1966, pp. 366-395.

12. Blodgett, Katharine B.; and Langmuir, Irving: Accommodation Coefficient of Hydrogen; A Sensitive Detector of Surface Films. Phys. Rev., vol. 40, no. 1, Apr. 1, 1932, pp. 78-104.

13. Messiah, Albert (G. M. Temmer, trans.): Quantum Mechanics. Vol. 1. Interscience Publ., 1961.

14. Goodman, F. O.: On the Trapping Process in Gas-Surface Interactions. Paper Presented at Sixth International Symposium on Rarefied Gas Dynamics, Massachusetts Inst. Tech., Cambridge, Mass., July 22-26, 1968.

15. Beder, E.: On the Total Force of Elastic Scattering-Neutral Particles and Perfect Crystal. Surface Sci., vol. 1, 1964, pp. 242-279.

16. Trilling, Leon: Thermal Accommodation of Rare Gases on Clean Metal Surface - Comparison of a Simplified Classical Lattice Theory with Experiments. Rarefied Gas Dynamics. Vol. 1. C. L. Brundin, ed., Academic Press, Inc., 1967, pp. 139-154.

17. Schiff, Leonard I.: Quantum Mechanics. Second ed., McGraw-Hill Book Co., Inc., 1955, p. 65.

BIBLIOGRAPHY

The following publications contain extensive references to previous research in gas-surface interactions, and therefore an exhaustive bibliography is not given here.

Flood, Edward A., ed.: The Solid-Gas Interface. Vols. 1 and 2. Marcel Dekker, Inc., 1967.

Hurlbut, F. C.: Current Developments in the Study of Gas-Surface Interactions. Rarefield Gas Dynamics. Vol. 1. C. L. Brundin, ed., Academic Press, Inc., 1967, pp. 1-34.

Stickney, R. E.: A Discussion of Energy and Momentum Transfer in Gas-Surface Interactions. Rep. AEDC-TR-66-13, Aro, Inc., Feb. 1966. (Available from DDC as AD-630522.)

Trilling, L.: Theory of Gas-Surface Collisions. Fundamentals of Gas-Surface Interactions. Howard Saltsburg, J. N. Smith, Jr., and Milton Rogers, eds., Academic Press, Inc., 1967, pp. 392-421.

"The aeronautical and space activities of the United States shall be conducted so as to contribute . . . to the expansion of human knowledge of phenomena in the atmosphere and space. The Administration shall provide for the widest practicable and appropriate dissemination of information concerning its activities and the results thereof."

— NATIONAL AERONAUTICS AND SPACE ACT OF 1958

NASA SCIENTIFIC AND TECHNICAL PUBLICATIONS

TECHNICAL REPORTS: Scientific and technical information considered important, complete, and a lasting contribution to existing knowledge.

TECHNICAL NOTES: Information less broad in scope but nevertheless of importance as a contribution to existing knowledge.

TECHNICAL MEMORANDUMS: Information receiving limited distribution because of preliminary data, security classification, or other reasons.

CONTRACTOR REPORTS: Scientific and technical information generated under a NASA contract or grant and considered an important contribution to existing knowledge.

TECHNICAL TRANSLATIONS: Information published in a foreign language considered to merit NASA distribution in English.

SPECIAL PUBLICATIONS: Information derived from or of value to NASA activities. Publications include conference proceedings, monographs, data compilations, handbooks, sourcebooks, and special bibliographies.

TECHNOLOGY UTILIZATION PUBLICATIONS: Information on technology used by NASA that may be of particular interest in commercial and other non-aerospace applications. Publications include Tech Briefs, Technology Utilization Reports and Notes, and Technology Surveys.

Details on the availability of these publications may be obtained from:

SCIENTIFIC AND TECHNICAL INFORMATION DIVISION
NATIONAL AERONAUTICS AND SPACE ADMINISTRATION
Washington, D.C. 20546